RSC Advances

ROYAL SOCIETY OF CHEMISTRY

www.rsc.org/advances

Cite this: DOI: 10.1039/c0xx00000x

www.rsc.org/xxxxxx

ARTICLE TYPE

Exploitation of surface acoustic waves to drive nanoparticle concentration within an electrification-dependent droplet

Zheng Tengfei,Wang Chaohui, Niu Dong, Jiang Weitao, Shi Yongsheng, Yin Lei, Chen Bangdao, Liu Hongzhong*, Ding Yucheng

State Key Laboratory for Manufacturing Systems Engineering, Xi'an Jiaotong University, Xi'an 710049, People's Republic of China
E-mail: hzliu@mail.xjtu.edu.cn

Ultrafast particle assembling plays an important role in subsequent analytical procedures and the development of miniaturized biological and chemical sensors. In this paper, standing surface acoustic wave (SSAW) devices are employed to drive nanoparticles in microlitre droplets with different concentrations of sodium chloride by exciting a MHz-order acoustic wave. Different patterns formed by particles are strongly dependent on the concentrations of sodium chloride. Two forces, i.e., dielectrophoresis (DEP) force generated by the alternating voltage, and fluid viscous drag force generated by the acoustic streaming, should dominate the particles assembling process, and induce various assembling patterns. The intricate and interesting interplay between fluid viscous drag force and dielectrophoresis (DEP) force on the particles is investigated in this study. We consider electric dipolar interaction to study behaviors of particles in droplets with different sodium chloride concentrations aroused by SSAWs. Theory analysis and experiments reveal that nanoparticles would form regular pattern only when the dielectrophoresis (DEP) decreased via increasing the conductivity of the droplet.

Introduction

Microfluidic systems on planar chips have gained popularity for handling miniscule volumes of liquids on the surface of open substrates. Open microfluidics offers a promising mode of digital microfluidics,[1] which involves micro/nano particles manipulation in droplets in a fast and economic route, avoiding specific functional components such as microchannels, pumps, valves, sorters. Handling liquid on open substrates also minimizes the contact between the fluid and the channel walls, thus decreases the risk of air-bubble clogging, fouling by debris and nonspecific surface adsorption of reagents. Sorting cells and biomacromolecules for the point-of-care diagnostics and the patterning of nanostructured materials are among the many emerging applications of submicron colloidal particle assembly.[2] In principle, an effective airborne microparticle sampling device should be able to collect and concentrate airborne microparticles into a carrier for subsequent detection downstream through a biosensor component. To date, many techniques such as magnetic,[3] optic,[4] dielectrophoretic,[5] and centrifugation methods,[6] have been proposed to manipulate particles and cells. However, there are some disadvantages adapting these methods, such as needing a complicated optical setup, damaging biological cells due to high heating, requiring of labeling of particles. Consequently, the development of a precise, easy, biocompatible, and label-free manipulation method is required.

Surface acoustic waves (SAWs) have proven to be a promising method for particle assembling and micro/nanostructure alignment. There has been much progress in controlling alignment of cells and microscale particles in droplets by SSAWs,[7-9] as mentioned previously. The behaviors of particles in droplets are complex because of existence of the acoustic streaming. Priscilla et al.[10], for the first time, demonstrates the existence of a frequency-dependent crossover particle size that can be used for effective particles partitioning. Li et al.[11] observes spatiotemporal patterns formed by colloids along the free surface of a drop beneath which SSAWs are applied.

Considering the particles in droplets driven by SSAWs, almost all the previous studies focus on the indirect drag force arising from acoustic streaming and the acoustic radiation force acting on the suspended particles.[12,13] Priscilla et al.[10] reveals that for a SSAW device with a certain frequency, there exists a critical size range, under which the particles are dominated by the drag force. In our paper, the size of the particles is smaller than the critical size range, so the particles are dominated by drag force. However, as the results of the piezoelectric effect and the inverse piezoelectric effect, a transient inhomogeneous electric field would be generated on the surface, while the SSAWs propagate along the free surface. The particles and the colloids, widely existing in chemical, biological and biomedical fields, will be acted by an electric field force[14,15] in a high-frequency electric field, besides the drag force arising from acoustic streaming. In earlier studies, acoustic radiation forces caused by pressure fluctuations in the liquid played a major role in the manipulation of microscale objects. Recently, a piezoelectric field induced by the SSAWs is used to align and pattern metallic nanowires by dielectrophoresis (DEP) in microchannels.[16-18] SSAWs induce an alternating electric field and create virtual electrodes[19] on a piezoelectric substrate. Chen et al.[18] manipulates nanowires in real time by controlling the distribution of the SSAW field.

In this paper, the role of the DEP force in the process of particles movement in a microlitre droplet is investigated. We demonstrate the complicated movement of particles in the droplet when SSAWs propagate into it. The experimental

results indicate that, a force (namely DEP force), caused by the electric field when SSAWs propagating, also contributes to the particle concentration. By decreasing DEP forces, particle lines are obtained. Further experiments and simulations are carried out to prove the effects of DEP force. This paper reveals the novel coupling of the DEP force and the drag force (arising from acoustic streaming) acting on a particle suspension to drive size-dependent spatial assembling and partitioning in a sessile droplet atop the substrate of a SAW device.

Experiments and Results

As shown in Figure 1(a), a drop containing an aqueous suspension of ϕ300 nm silicondioxide particles is placed on the substrate entirely within the SAW propagation path. The SAW is a Rayleigh wave[20] generated by a sinusoidal electric potential applied to an interdigital transducer (IDT) on the surface of a lithium niobate(LN) single-crystal piezoelectric substrate. Figure 1(b) illustrates the displacement of the substrate induced by the SAW. Figure 1(c) illustrates the potential induced by the inverse piezoelectric effect when the shape of the piezoelectric substrate changed.

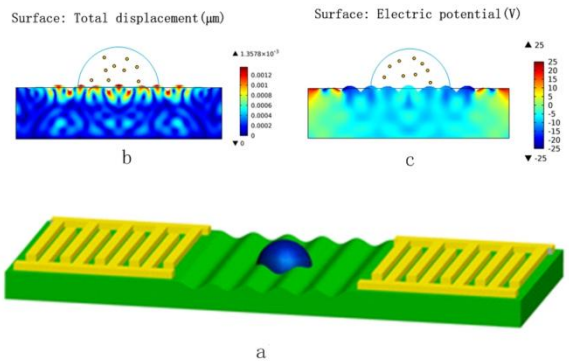

Figure 1. Schematic of the SSAW propagating process. (a)Schematic of the SAW device. The propagating SAW wavelength is defined by the IDT finger width and spacing, both of which are λ/4. A droplet is placed on the substrate entirely within the SAW propagation path. (b) The displacement of the substrate induced by the SAW. (c) The potential induced by the change in shape of the piezoelectric substrate.

A SSAW device has been fabricated to investigate the electric field force generated by the inverse piezoelectric effect. The device consists of a lithium niobate substrate and two dual layer interdigital transducers (IDTs). The dual layer (Al/Cr) IDTs comprise straight finger pairs (typically 20) and are actuated at its characteristic resonant frequency (at 2.8 MHz). A voltage (25V) is supplied to the SAW device (the voltage is generated by a signal generator (AFG3022, USA) and amplified by an amplifier (TREK MODEL 2100HF)), and measured by a digital oscilloscope (Tektronix TDS3014B, USA). The silica particles are synthesized by the classical Stober method. The hydrolysis of tetraethyl orthosilicate in the chemical reaction induces the adsorption of hydroxyl on the particle/liquid interface, resulting in an increase in the surface conductance to approximate 0.18 S/m. The silica particles were then suspended in aqueous solution at individual concentration on the order of 10^6 particles/mL. The assembling behaviors of the particles in the microlitre droplet are observed by a microscope (Nikon eclipse LV100, Japan).

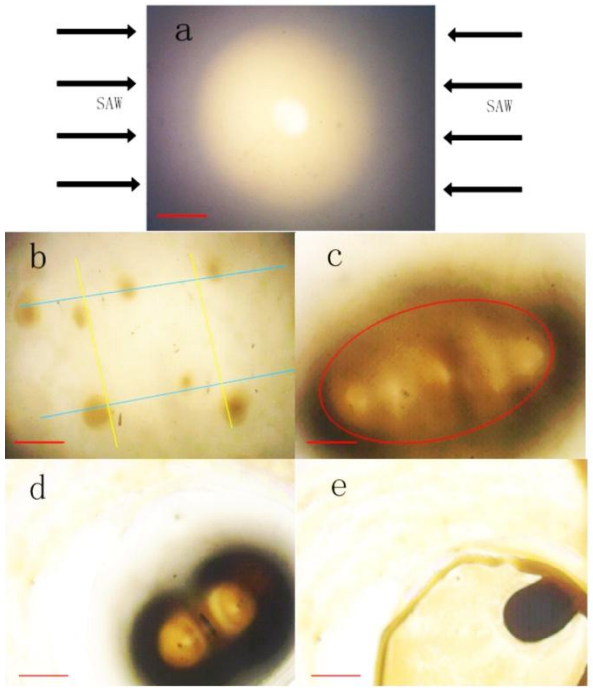

Figure 2. The assembling process of nanoparticles in a deionized water droplet and the scale bar is 500 μm. (a) Particles distribute in a droplet uniformly before the SSAWs are applied. (b) Particles cluster into islands in the center of the droplet once SSAWs are actuated. Blue lines indicate the electric field direction, and the yellow lines indicate the antinodes of the SSAWs. The main particle islands emerge in the crossing points of the field lines and the wave antinodes. (c) With the fraction decreasing of water by evaporating, a baseball shape is formed by particles clustering. (d) Particles in the drop are collected to a double-pointed pattern. (e) Along with water evaporation, the acoustic streaming gradually decreases and finally disappears, resulting in particles assembling to an island.

Figure 2 illustrates the assembling process of nanoparticles in a deionized water droplet. As shown in Figure 2(a), Particles distribute uniformly in a droplet before the SSAWs are applied. Figure 2(b) shows that particles cluster to islands around the center of the droplet when SSAWs are applied, which is accompanied by low frequency sub-harmonic oscillations on the free surface of the droplet.[11] Given that the SSAWs excitation power is kept constant and the drop is free to evaporate, by reducing the droplet volume, the amount and the positions of islands mutate subsequently. As a result, the concentration of the particles in the droplet is observed, as demonstrated in Figure 2(c). After the drop volume decreased to a particular value, particles in the drop are collected to a double-pointed pattern, as showed in Figure 2(d). The flow in the droplet, induced via acoustic streaming, attenuates along with the evaporation. And particles assemble in an island. Figure 2(e) shows the assembling and partitioning of the particles in the drop.

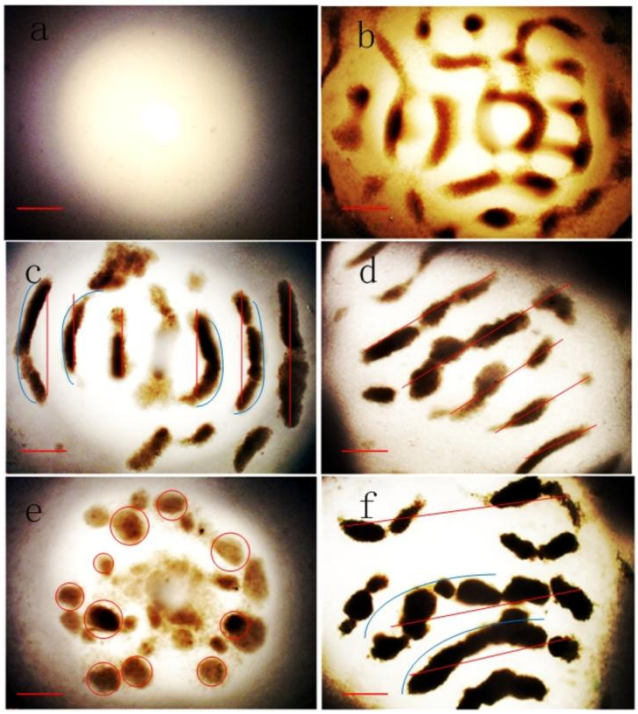

Figure 3. The assembling process of nanoparticles in the droplet with the sodium chloride concentration of 0.144 g/mL and the scale bar is 500 μm. (a) Particles distribute in the droplet uniformly before the SSAWs are applied. (b) Particles gather in short chains. (c) Particles assemble in lines perpendicular to the SAW wave line. The red lines indicate particles gather in lines, and blue curves indicate the curling particle chains. (d) Particles lines are moving from the direction perpendicular to SAW propagation to that having an angle with the electric field line by increasing $\boldsymbol{F_{DEP}}$. The red lines indicate the direction of the particle chains. (e) Particle chains are broken up to form islands in the droplet with further increasing of $\boldsymbol{F_{PDE}}$. (f) The $\boldsymbol{F_{DEP}}$ dominates the behaviors of particles concentration, and particles gather in lines along the electric field line when the distance between particles and the substrate decreases to short enough.

Particles experience a complex motion when SSAWs are applied. The motion of particles in the droplet has been studied in previous works. However, the behaviors of the particles in ions solution have rarely been investigated. Figure 3 illustrates the particle behaviors in the droplet of sodium chloride (0.144 g/mL in concentration). As shown in Figure 2(a), particles distribute in a droplet uniformly before the SSAWs are applied. Figure 3 (b) shows the performance of the particles when the SSAWs are applied. Besides particles moving in cycles, most of the particles, dominated by the drag force, gather in chains located in the cycles. Then, the particles rings are broken up by the drag force and most particles are aligning along lines perpendicular to waves propagating direction (Figure 3(c), (d)). With further evaporation, the distance between the particles chains and the substrate surface diminishes, resulting in the $\boldsymbol{F_{DEP}}$ increasing. Therefore, the particles chains rotate within the droplet. When the direction of the particle chains has an angle with the electric field lines, the chains are in an instant stable state balance of the drag force and the DEP force, as demonstrated in Figure 3(d). Once the drop volume decreases to a certain value, the magnitude of the DEP exceed the drag force. The particle chains are dominated by the DEP force to align with the electric field (Figure 3(f)). At first, particle chains are broken up and formed many particle islands distributing uniform within the drop. Then particle islands are moved to line up along the electric field lines and the wave propagation direction (Figure 3(e) (f)).

DISCUSSION

Many researchers have exploited the mathematical modeling and numerical simulation of the acoustic streaming and acoustic radiation acting on particles.[21-23] In the journal of Lab on a Chip, there is a thesis about acousticofluidics, and there are several papers referring to the applied of the SAW.[12,13,24] Recently the group of Henrik have published a paper about the motion of microparticles in three dimensions induced by ultrasound.[25] Alghane et al.[21]simulated the vortexes in the drop aroused by SAW. However, in this paper the droplet was assumed to be confined with a rigid boundary. Those papers almost all neglect the $\boldsymbol{F_{DEP}}$ induced by the SSAWs. DEP is the movement of a charge neutral particle in a dielectric fluid induced by an inhomogeneous electric field.[26-28] Recently, the $\boldsymbol{F_{DEP}}$ induced by SSAWs are used to pattern nanowires.[16-18] However, the theory of particle behavior is complex due to the very intricate and interesting interplay of physics of fluid viscous drag and the DEP force on the particles within a droplet. So far, the exact behavior of particles driven by SSAWs is unknown and further research should be designed to evaluate the theory of expressing the phenomenon of particles in a droplet induced by SSAWs.

In our experiment, a similar phenomenon as that reported by Li et al.[11] is observed at first. When deionized water is replaced by sodium chloridesolution,however, particles begin to gather in lines perpendicular to the propagation direction of the SAW, and the behavior of gathering in lines is enhanced as the sodium chloride concentration increasing. The standing mechanical vibration induces an alternately charge distribution on the $LiNbO_3$ substrate. The periodic distribution of electric charges, which is determined by SSAWs pressure antinodes, generates an AC electric field with electric field lines from positive charges to negative charges, and induces DEP force on the neutrally particles in the electric field. The DEP force has been used to align nanowires in the micro channel.[16-18] The force on an induced dipole can be described as $F \propto (p \cdot \nabla)E$, where p is the dipole moment and E is the electric field.[26] When deionized water was replaced by sodium chloridesolution, the conductivity of the solution increased while the in-phase particle polarizability decreases.[29,30] As a result, the DEP force decreases and the drag force dominates the movement of particles. Under the impact of the drag force, particles align in lines. To further study the functions of the DEP force and the drag force, an experiment about acoustic streaming and a simulation about DEP (Fig.4) are employed.

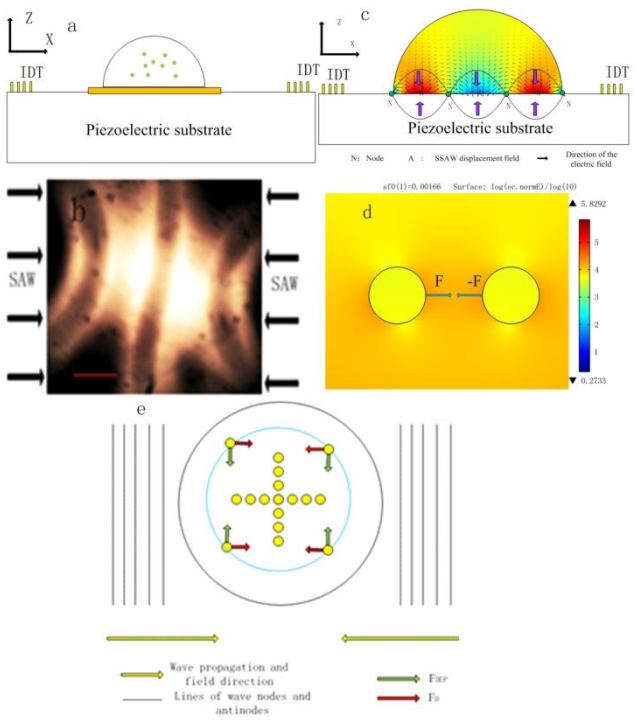

Figure 4. (a) Schematic of SAW device. Au layer is deposited on $LiNbO_3$ substrate and supports particle suspension droplet.(b) Particles assemble in lines perpendicular to the SAWs propagating line. The scale bar is 500 μm. (c) Cross-section view of IDT-deposited piezoelectric substrate along x axis. The mechanical vibration of the substrate is induced by SSAWs, and the electric field is generated by non-uniform charge distribution. The up part shows the simulation of the electric field distribution in the droplet. (d) Simulation result of electric field around the two nanoparticles. The arrows show the direction of $\boldsymbol{F_{DEP}}$ acting on particles. (e) Nanoparticles are suffered two forces: the drag force ($\boldsymbol{F_D}$) arising from acoustic streaming, and the DEP force ($\boldsymbol{F_{DEP}}$) due to the Maxwell-Wagner interfacial charge relaxation. $\boldsymbol{F_D}$ drives the particles to gather in lines perpendicular to the waves propagating direction, and $\boldsymbol{F_{DEP}}$ arranges the particles in chains aligned along the electric field.

In order to deeply understand the role of the drag force, further experiment is carried out by introducing a layer of coupling liquid (water) and an Au layer between the $LiNbO_3$ substrate and the particle suspension droplet (Figure 4(a)). The Au layer is designed to shield the particles from the electric field. As a result, the DEP force is significantly screened, whereas the SSAWs could still transmit into suspension. When a liquid droplet lies in the path of a SAW, the wave changes its mode to a leaky surface acoustic wave (LSAW) when it reaches the boundary between solid and liquid. The attenuation of the LSAW, due to viscous liquid loading, transfers a drag force into the droplet, resulting in a significant movement to the nodes in the droplet. Finally, particles assemble in lines perpendicular to the SAW wave line (Figure 4(b)).

An electric field with frequency at MHz, which is generated on the surface while the SSAWs propagate on it, is exerted on the droplet. An alternating electric field hence exists in the liquid droplet, in which the field intensity attenuates with the increasing distance from the substrate surface. Since the conductivity of the particles is higher than its surroundings in the experimental conditions, they move closer to the chip substrate under the guidance of DEP force. Simultaneously, a near-field DEP attraction force would play its dominant role on particle chaining along the field lines once an appropriate particle concentration is applied.[31]Therefore, the multiple activities of particles in the droplet are caused by the drag force and the DEP forces.

The periodic distribution of electric charges generates an electric field. To further study the forces exerted on nanoparticles, the electric field was simulated using COMSOL Multiphysics 4.3a software (Figure 4(c)). The bottom part shows the vibration and potential of the lithiumniobate. The up part shows the electric field in the droplet induced by the surface potential. The black arrows indicate that the field lines are parallel to the propagation direction of the SSAWs. When an electric field is imposed on suspension, the particles are polarized and a non-uniform induced free charge distribution accumulates at the particle surfaces. If further under the influence of a background field gradient, the DEP and the near-field DEP interaction force, acting on these interfacial dielectric gradients, would push nanoparticles in chain configuration with a parallel orientation to the local field lines. The simulation result shows that particles have the trend to line along the propagation direction of SAW (Figure4 (d)).

The behavior of the particles is caused by the different orientations of the drag force and the DEP force acting on the particles (see Figure 4(e)). As the SSAWs radiate into the droplet at the Rayleigh angle, the drag force, induced by the acoustic streaming, acts on the particles to drive them toward lines perpendicular to the SAW wave line, while the DEP force drives them toward the field lines. Under the combining effects of those two forces, most particles circulate within the droplet, except a few particles that locate in the crossing points of the field lines and the wave antinodes (see Figure 2(b)). With the volume fraction of water decreasing in the evaporation process, the distance between the particles and the substrate reduces and the DEP force acting on particles increases. The intensive DEP force drives the particles to line up along the electric field line. As a result, particles form a baseball shape (see Figure 2(c)). After the volume of the drop decreased to a certain value (see Figure 2(d)), the area contained by the droplet is decreasing. The gradient of electric field diminishes and the DEP force decreases too, which leads to particles gathering in a double-pointed pattern (see Figure 2(d)). Under the multiple effects of the acoustic fluid drag force and the DEP force, a double vortex flow pattern is produced in the droplet. To balance those forces, the vortexes locate at the line making angles with both the field lines and the wave antinodes. This arrangement is unstable not only for drag force but also for DEP force. Finally, the drag force disappears as the evaporation is continuous, particles around vortexes are broken up and gathering in an ellipse, aligning with the electric field line (see Figure 2(e)).

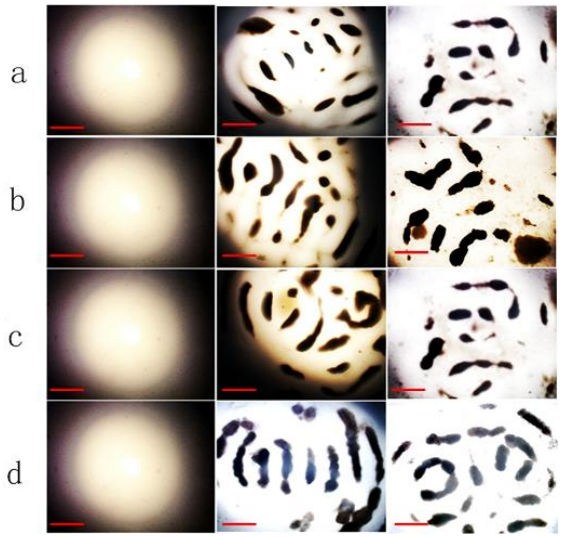

Figure 5. The assembling process of nanoparticles in the droplet with varying sodium chloride concentrations. The scale bar is 500 μm. (a) 0.009 g/mL. (b) 0.027 g/mL.(c) 0.045 g/mL (d) 0.072 g/mL. The average length of particle chains increases with the decreasing of the $\boldsymbol{F_{DEP}}$, when the concentration of the sodiumchloride arises from 0.009 g/mL to 0.072 g/mL.

When the deionized water is replaced by sodium chloride solution, the DEP force decreases due to the decreasing in-phase induced polarizability in high conductivity solution.[29.30]The drag force dominates the movement of particles to form a regular pattern(see Figure 3(b), (c)). In the process of evaporation, the behaviors of particles are complicated. Since the distance between the particles chains and the substrate surface cuts down, the DEP force increases. Therefore, a trend can be clearly observed that particles try to align along the propagation direction of SSAWs (see Figure 3(d)(e)(f)), which can be further proved by changing of the sodium chloride concentration. The experiment results are demonstrated as Figure 5. In Figure 5(a), only a few particles assemble in several islands, and those islands locate in circles formed by the combining effect of the drag force and the DEP force. With the decrease of DEP forces on account of higher conductivity, the length of particle chains increases and the new balance of the two forces makes the chains to align in lines having an angle with electric field line, as Figure 5(b), (c), (d) show. When the concentration rises up to 0.144 g/mL, most particles gather in lines perpendicular to the propagation direction of waves in Figure 3(c). With the process of evaporation, the distance between the chains and the substrate surface diminishes. The DEP force $\boldsymbol{F_{DEP}}$, due to the Maxwell-Wagner interfacial charge relaxation, dominates the particles movement. Finally, particles gather in line along the electric field line. The length of the particle chains, perpendicular to the wave propagation direction, depends on the magnitude of the $\boldsymbol{F_{DEP}}$. Figure 6 shows the $\boldsymbol{F_{DEP}}$ dependence of the average length of particle chains, when the concentrations of the sodiumchloride arise from 0.009 g/mL to 0.144 g/mL.

The experimental results revel that, DEP force acting on particles exists when the SAW is applied in the fluid. The DEP force, induced by the inhomogeneous electric field arising from the inversepiezoelectriceffect, enormously complicates the particles behaviors in the droplet. In order to manipulate nanoparticles in a droplet, more attention should be paid to the DEP force induced by SAW in the droplet.

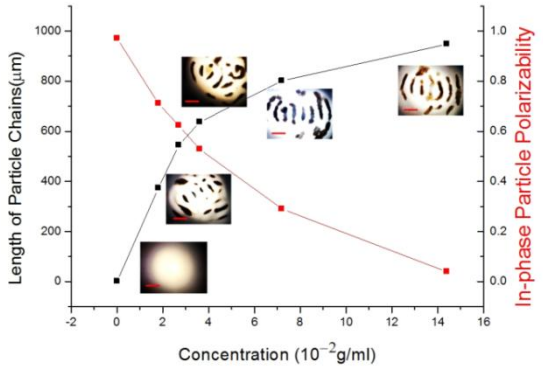

Figure 6.The length of particle chains and the in-phase particle polarizability in different sodium chloride concentrations. The scale is 500 μm. The blue line indicates the average length of particle chains increase when the concentration of the sodium chloride arise from 0 to 0.144 g/mL. The red line indicates that in-phase particle polarizability decreases when the concentration of the sodiumchloride arises from 0 to 0.144 g/mL. $\boldsymbol{F_{DEP}}$ is proportional to the in-phase particle polarizability. The pictures show particle behaviors in the NaCl concentration of 0, 0.036 g/mL, 0.072 g/mL and 0.144 g/mL.

4 CONCLUSION

In this paper, different behaviors of nanoparticles gathering in droplets(sodium chloride solution)actuated by SSAWs are deeply investigated. Via the DEP effects, the gathering behaviors can be explained reasonably. Two forces, namely the DEP force arising from dielectrophoresis and the drag force arising from acoustic streaming, are always coupled and exploited to manipulated nanoparticle movements in circles. Generally, different magnitudes of the DEP force within droplets, result in different performance of particles in the experiment. Accordingly, these forces are obtained and exploited to manipulate nanoparticles in a microlitre droplet using a 2.8MHz SSAW device. By manipulating the magnitudes of the DEP forces related to the concentration of ions, various patterns of the nanoparticles gathering can be formed. In order to manipulate nanopaticles and micro-particles in droplets and microchannels accurately, manipulating of the DEP forces, related to the size of particles, the frequency of the SAW and the conductivity of the medium, is deserved to deeply investigated. This research would promote the application of SAW in ultrafast concentration and partitioning of cells and biomolecules in discrete fluid systems, which is essential for diagnostic procedures such as analytical detection.

ACKNOLEDGMENTS

This work is supported by the Major Research Plan of Nationa l Natural Science Foundation on Nanomanufacturing (No. 913

23303), National Natural Science Foundation of China (No. 51275400), National Science and Technology Project (Nos. 2011ZX04014-071, SK201401A53-01, CERS-1-X1),theFundamental Research Funds for the Central Universities, and China Postdoctoral Science Foundation (Nos. 2012M520081, 2013M530419, 2013M530424, and 2013M532035)and we thank doctor Weiyu Liu for valuable discussions on this subject.

References

1 K. Choi, A. H. Ng, R. Fobel and A. R. Wheeler, Annu. Rev.Anal.Chem., 2012, 5, 413-440.
2 E. Kim, Y.Xia and G. M. Whitesides, Nature (London), 1995, 376,581.
3G.Degre, E. Brunet, A. Dodge and P. Tabeling, Lab Chip, 2005, 5, 691-694.
4 J. Enger, M. Goksor, K. Ramer, P. Hagberg and D.Hanstorp, Lab Chip, 2004, 196-200.
5 T. Muller, A. Pfenning, P.Klein, G. Gradl, M. Jager and T. Schnelle, IEEE Eng. Med. Biol. Mag., 2003, 22, 51-61.
6 J. Seo, M. Lean and A. Kole, Appl. Phys. Lett., 2007, 91, 033901.
7 M. Tan, J. Friend and L. Yeo, Lab Chip, 2007, 7, 618-625.
8 C. D. Wood, S. D. Evans, J. E. Cunningham, R. O. Rorke, C. Walti and A. G. Davies, Appl. Phys. Lett., 2008, 92, 044104.
9 Richie J. Shilton, Marco Travagliati, Fabio Beltram and Marco Cecchini, Advanced Materials, 2014, 201400091.
10 Priscilla R. Rogers, James R. Friend and Leslie Y. Yeo, Lab Chip, 2010, 10, 2979-2985
11 HaiYan Li, James R. Friend and Leslie Y. Yeo, Physical Review Letters, 2008, 101, 084502.
12 Martin Wiklund, Roy Green and MathisaOhlim, Lab Chip, 2012, 12, 2438-2451.
13Richie J. Shilton , Marco Travagliati , Fabio Beltram , and Marco Cecchini, Adv. Mater. 2014,201400091.
14 J. R. M and G. I. Taylor, Annual Review of Fluid Mechanics, 1, 111-146.
15 Michael C. Breadmore, Mohamed Dawod and Joselito P. Quirino, Electrophoresis, 2011, 32, 127-148.
16 C. J. Strobl, C.Schaflein, U. Beierlein, J. Ebbeckea and A. Wixforth, Appl. Phys. Lett., 85, 1427-1429.
17 X. H. Kong, Ch. Deneke, H. Schmidt, D. J. Thurmer, H. X. Ji, M. Bauer and O. G. Schmidt, Appl. Phys. Lett., 2010, 96, 134105.
18 Yuchao Chen, Xiaoyun Ding, Sz-Chin Steven Lin, Shikuan Yang, Po-Hsun Huang, Nitesh Nama, Yanhui Zhao, Ahmad Ahsan Nawaz, Feng Guo, Wei Wang, YeyiGu, Thomas E. Mallouk and Tony Jun Huang, ACS NANO, 2013, 7, 3306-3314.
19 A. Jamshidi, P. J. Pauzauskie, P. James Schuck, A. T. Ohta, P. Y. Chiou, J. Chou, Peidong Yang and Ming C. Wu, Nature Photonics, 2008, 2, 86-89.
20 White R. and Voltmer F, Appl. Phys. Lett., 1965, 7, 314-316.
21 M Alghane, B X Chen, Y Q Fu, Y Li, J K Luo and A J Walton, J.Micromech. Microeng, 2011, 015005(11pp).
22 Leslie Y. Yeo and James R. Friend, Annual Review of Fluid Mechanics, 2014, 46, 379-406.
23 X Y Du, M E Swanwick, Y Q Fu, J K Luo, A J Flewitt, D S Lee, S Maeng and W I Milne, J. Micromech. Microeng., 2009, 19, 035016(10pp).
24 Andreas Lenshof, Cecillia Magnusson and Thomas Laurell, Lab Chip, 2012, 12, 1210.
25 P. B. Muller, M.Rossi, A. G. Marin, R. Barnkob, P. Augustsson, T. Laurell, C. J. Kahler and H. Bruus, Physical Review E, 2013, 88, 023006.
26 H. A. Pohl, J.Appl. Phys., 1951, 22(7), 869-871.
27 Pohl. H. A, J. Appl. Phys., 29(8), 1182-1188.
28 X B Wang, Y Huang, F F Becker and P R C Gascoyne, J. Phys. D: Appl. Phys., 1994 27, 1571-1574.
29 Liu W. Y., Ren Y. K., Shao J. Y., Jiang H. Y., Ding Y. C., J. Phys. D: Appl. Phys, 2014, 47, 075501(15pp).
30 P Garcia- Sanchez, Ren Y K, Arcenegui J J, Morgan H and Ramos A, Langmuir, 2012, 28, 13861-13870.
31 Haitao Ding, Weiyu Liu, Jinyou Shao, Yucheng Ding, Liangliang Zhang and JiqiangNiu, Langmuir, 2013, 29, 12093-12103.

